P Allotropes

DOI: 10.1002/anie.201404147

The Extended Stability Range of Phosphorus Allotropes**

*Frederik Bachhuber, Jörg von Appen, Richard Dronskowski, Peer Schmidt, Tom Nilges, Arno Pfitzner, and Richard Weihrich**

Dedicated to Professor Martin Jansen on the occasion of his 70th birthday

Abstract: *Phosphorus displays fascinating structural diversity and the discovery of new modifications continues to attract attention. In this work, a complete stability range of known and novel crystalline allotropes of phosphorus is described for the first time. This includes recently discovered tubular modifications and the prediction of not-yet-known crystal structures of [P_{12}] nanorods and not-yet-isolated [P_{14}] nanorods. Despite significant structural differences, all P allotropes consist of covalent substructures, which are held together by van der Waals interactions. Their correct reproduction by ab initio calculations is a core issue of current research. While some predictions with the established DFT functionals GGA and LDA differ significantly from experimental data in the description of the P allotropes, consistently excellent agreement with the GGA-D2 approach is used to predict the solid structures of the P nanorods.*

Red and red-brown fibers of recently described allotropes of phosphorus instigated subsequent investigations. How should they be classified in the known stability range of white, red, and black phosphorus (see Figure 1 a),[1] which can be used as a model in the search for new metastable compounds?[2] Structure–property relations and compliance with Ostwald's rule become apparent. Accordingly, the reactive white form of phosphorus discovered by Brand back in 1669 corresponded to a metastable product.[1] Today we know three modifications of white phosphorus (α-, β-, and γ-P_4).[3] As in the gas phase, they consist of tetrahedral P_4 units and they differ by a distinct arrangement of the tetrahedra.

Orthorhombic black phosphorus (*o*-P),[4] considered to be the thermodynamically stable allotrope, is formed under pressure. Direct access was not possible until a few years ago with the aid of the mineralizator concept.[5] *o*-P consists of layers of six-membered rings similar to the trigonal high-pressure form (*h*-P)[6] that exhibits the structure of gray arsenic, but *o*-P differs in terms of the interconnection of the six-membered rings. At even higher pressures, a simple cubic three-dimensionally (3D), covalently linked structure of the α-Po-type (*c*-P) evolves. When white phosphorus is heated to more than 200 °C, a gradual transition to amorphous and crystalline forms of red phosphorus can be observed.[1] They are based on tubular units of five- and six-membered rings (as shown below). As their structures were not known, the various red forms were initially numbered as I–V.[7] For a long time, modification V, known as violet Hittorf's phosphorus (monoclinic, *m*-P), was the only structure that could be refined. It crystallizes as plates from white P in molten lead which were characterized by Thurn and Krebs.[8]

In the last decade, Pfitzner et al.[9] and Ruck et al.[10] managed to synthesize further tubular P allotropes. Red, fibrous phosphorus crystals (triclinic, *t*-P) were obtained in addition to *m*-P at 570–590 °C from amorphous red phosphorus. The diffraction pattern of fibrous phosphorus corresponds to that of the crystalline red form IV. The structure solution confirmed the assumption that *t*-P is built of the same tubes that occur in *m*-P but arranged as parallel sets of covalently linked rods instead of layers of orthogonally linked rods. Pfitzner et al. prepared two novel solid red-brown P allotropes[9] from the adduct compounds $(CuI)_8P_{12}$[11] and $(CuI)_3P_{12}$.[12a] According to TEM investigations, they contain isolated P nanorods, which are arranged in parallel in the solids. Suspected relaxation effects, structures, and stabilities could not be determined accurately. Another form of nanorods occurs in $(CuI)_2P_{14}$[12b] but this compound has not yet been prepared in a pure state. Nanorods were simultaneously predicted by Häser et al.[13] and described as [P8]P4(4)[(*n*1), [P10]P2 (*n*2), and [P12(4)]P2[(*n*3) according to Baudler's rules.[14] Häsers quantum chemical calculations proposed the nanorods as well as Hittorf's phosphorus and fibrous phosphorus to be similarly stable in terms of their structural units, but did not provide information about the stability order of the solid-state structures. Remarkably, the rather unexpected linkage of P_8 cages via P_4 rings in [P8]P4(4)[appears to be an energetically favorable alternative to P_5 rings. According to recent in situ gas-phase studies, fibrous phosphorus is more stable than the black allotrope at 400–500 °C and Hittorf's phosphorus, on the other hand, is less stable.[15] Does this mean that the stability order of P allotropes has to be

[*] F. Bachhuber, Prof. Dr. A. Pfitzner, Priv.-Doz. Dr. R. Weihrich
Institut für Anorganische Chemie, Universität Regensburg
Universitätsstraße 31, 93040 Regensburg (Germany)
E-mail: Richard.weihrich@ur.de
Homepage: http://www.uni-regensburg.de/chemie-pharmazie/anorganische-chemie-weihrich/index.html
Dr. J. von Appen, Prof. Dr. R. Dronskowski
Institut für Anorganische Chemie, RWTH Aachen University
Landoltweg 1, 52056 Aachen (Germany)
Prof. Dr. P. Schmidt
Fakultät für Naturwissenschaften, BTU Cottbus-Senftenberg
Großenhainer Straße 57, 01968 Senftenberg (Germany)
Prof. Dr. T. Nilges
Department of Chemistry, TU München
Lichtenbergstraße 4, 85747 Garching (Germany)

[**] R.W., P.S., R.D. und T.N. kindly thank the DFG for financial support in the framework of the priority project SPP 1415.

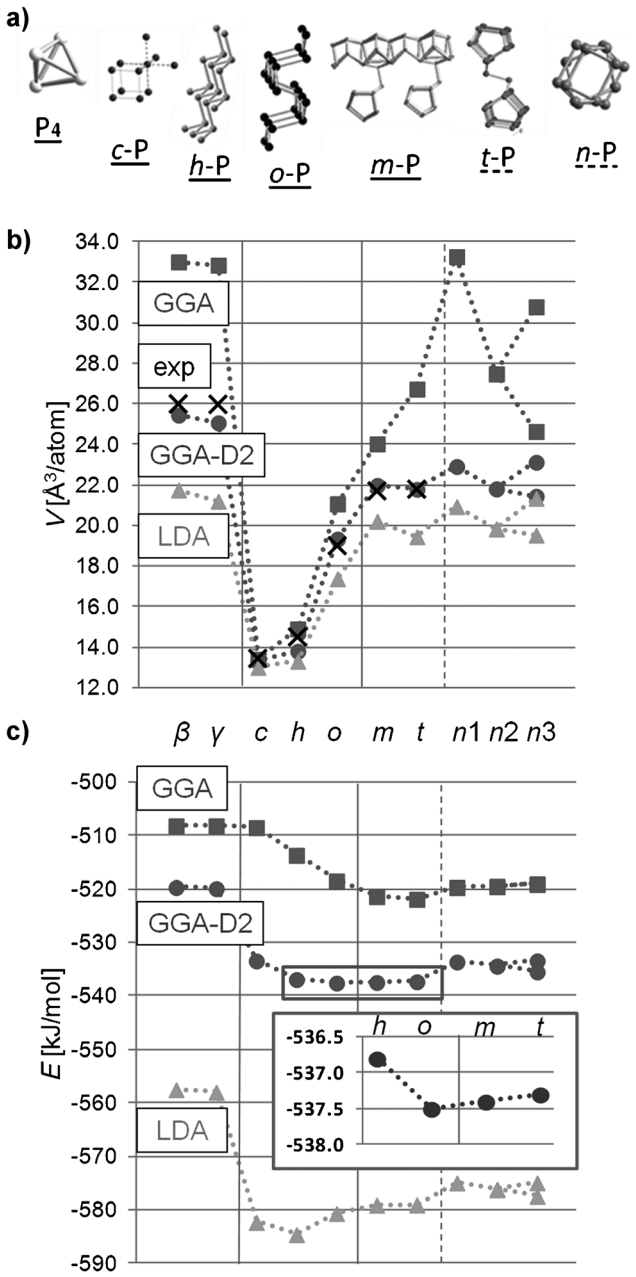

Figure 1. a) P allotropes (covalently linked structural units) of the β and the γ modifications of white P; cubic *c*-P, gray *h*-P, black *o*-P, violet *m*-P, red fibrous *t*-P as well as *n*-P nanorods (cf. main body). b) Calculated cell volumes according to LDA, GGA, and GGA-D2 methods ($T = 0$ K). ■: GGA, ×: exp., ●: GGA-D2, ▲: LDA. c) Calculated cohesive energies; the inset highlights the energetic order of energetically similar allotropes according to GGA-D2.

rewritten? Where are Pfitzner's nanorod allotropes located in this series?

To answer these questions, we calculated the binding energies of crystal structures of known and new P allotropes on the Born–Oppenheimer energy surface ($T = 0$ K). Covalent and intermolecular interactions were addressed by different approaches, and the results show a systematic but surprisingly high influence of van der Waals forces. Similar to the energetic situation of carbon nanotubes relative to graphite and diamond, the tubular 1D P nanorods can be classified between molecular (P_4, 0D), layered (*o*-P, *t*-P, 2D), and covalently linked (*c*-P, 3D) structures.

If one first considers the cell volumes of all P allotropes (Figure 1 b), they are systematically over- and underestimated with DFT-GGA and DFT-LDA calculations, respectively. Deviations from the experiment become more pronounced with an increasing contribution of noncovalent interactions ($P_4 > t$-P $> o$-P $> m$-P). They are responsible for bonding between P_4 molecules in white phosphorus, the layers in *o*-P, and the polymers in the tubular forms. Unfortunately, they are intrinsically not described (GGA) or overestimated (LDA) by standard DFT methods. The smallest deviations of calculated and experimental values are thus found for the high-pressure phases. With the aid of the dispersion-correction GGA-D2,[16] however, cell volumes of all P allotropes are well reproduced within the usual tolerance for DFT (< 1% per lattice parameter). The largest effect of the dispersion correction on the cell volume is found for white and fibrous phosphorus. Similar packing effects are predicted for the nanorods.

Significantly varying results are obtained for the stabilities as well (Figure 1 c). If one takes only covalent interactions (GGA) into account, *o*-P is described to be more stable than its high-pressure phases (about 5 and about 10 kJ mol^{-1}, respectively). Surprisingly, all tubular allotropes (including the nanorods) are predicted to be a few kJ mol^{-1} lower in energy than *o*-P. The isolated covalent structural units of *t*-P and *m*-P hence appear to be more stable than the nanorods and the layers realized in *o*-P. Only the consideration of the interactions between the structural units changes this order. Their overestimation with the LDA functional leads to an immoderate preference of the high-pressure forms. In contrast, when the GGA-D2 correction term is used, orthorhombic black phosphorus represents the lowest in energy on the potential energy surface at $T = 0$ K, closely followed by the tubular allotropes. Hittorf's P is located only about 0.1, fibrous P about 0.2, and the high-pressure form *h*-P about 0.7 kJ mol^{-1} higher in energy. The calculated difference between *o*-P and the crystalline allotropes of white P (β and γ) is about 17 kJ mol^{-1}. This value is within the range of the rather limited experimental data available for P, such as the transitions P(white)→P(red) (-17.6 kJ mol^{-1})[17] and P-(white)→P(black) (-21.2 ± 2.1 kJ mol^{-1}).[18] The deviations indicate temperature effects and so does the measured increase in stability of *t*-P at $T > 400$ °C.[15]

Solid crystalline structures of P nanorods are predicted for the first time and they are integrated into the stability row at about 5 kJ mol^{-1} above black P. Consequently, they are considerably more stable than white phosphorus. Among the nanorod allotropes, the stability decreases from [P8]P4(4)[to [P10]P2[. The fact that the opposite trend is found for the GGA calculations implies that van der Waals forces largely determine the arrangement of the molecular units in the crystal structure. While they usually make up only a small part of the total binding energy in the solid state, van der Waals interactions determine the stability order for the P-allotropes. Calculations on not-yet-isolated [P12(4)]P2[reveal a stability comparable to the other rodlike structures

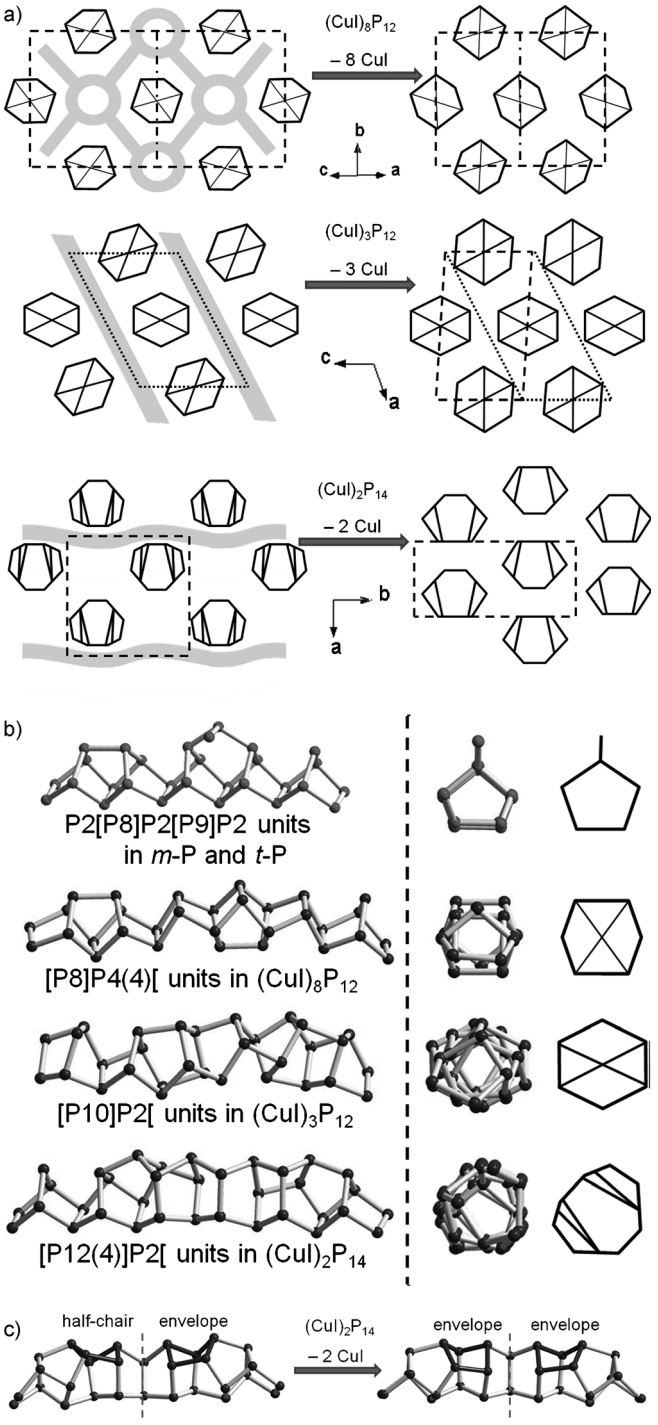

Figure 2. a) P nanorods in CuI matrices and predicted configurations after removal of the matrices (unit cells are indicated by dashed lines). b) Structural fragments of *m*-P, *t*-P, and P nanorods (left: side view, right: top view). c) Structural changes in $(CuI)_2P_{14}$ before (left) and after (right) the optimization.

and in addition a rearrangement within the arrangement of P atoms is observed (see below).

To obtain the solid-state structures of the nanorod allotropes, Cu and I atoms were removed from the simulation cells—in analogy to the experimental extraction of the P nanorods from CuI matrices (see Figure 2a, gray bars correspond to CuI matrices). This basically results in changes of the rod packings. CuI matrices separate the P rods in such a way that these are tetragonally ordered in $(CuI)_8P_{12}$ and $(CuI)_2P_{14}$, and hexagonally ordered in $(CuI)_3P_{12}$. After the CuI matrices are removed, the phosphorus polymers appear in hexagonal packings in all cases. A comparison of the structures with and without CuI matrices reveals that rotation and reorganization of the strands becomes more pronounced with a lower degree of preorganization by intermolecular contacts of the strands in the parent structures. This is most apparent for [P8]P4(4)[in $(CuI)_8P_{12}$, in which the P strands are completely separated by CuI. In $(CuI)_3P_{12}$, however, the layered arrangement of CuI and [P10]P2[polymers leads to a certain degree of preorientation. The driving force of the reorganization is the energetic optimization of the structure by means of a close packing of the polymers. This step is mainly dependent on van der Waals forces.

The projections in Figure 2b are described in terms of polyhedral units and bridging links as suggested by Häser using Baudler's notation.[13,14] *t*-P and *m*-P likewise consist of repeating units]P2[P8]P2[P9] with P_8 and P_9 cages that are connected by P_2 dumbbells. In addition, the strands are covalently linked; either orthogonal (*m*-P) or in parallel pairs (*t*-P). Interlinked five-membered rings can be recognized in the top view (Figure 2b, right). Nanotubes with P_8, P_{10}, and P_{12} cages appear in the repeating units [P8]P4(4)[, [P10]P2, and [P12(4)]P2[that are related to $(CuI)_8P_{12}$, $(CuI)_3P_{12}$, and $(CuI)_2P_{14}$.

For the strands isolated from $(CuI)_8P_{12}$ and $(CuI)_3P_{12}$, no changes in the polymer structures but changes in their orientation with respect to the previous matrix environment are predicted. In $(CuI)_2P_{14}$, the relatively low content of CuI leads to a high degree of preorganization. The reorientation effect achieved by the extraction of the P nanorods is thus very low. In contrast, the predicted polymer structures of [P12(4)]P2[diverge before and after the extraction. Two different data points for [P12(4)]P2[in Figure 1b and 1c (*n*3) correspond to two different packing motifs that are related to the change in the polymer structure. The obtained distortion is accompanied by a significant energy gain and explains a hitherto unsolved peculiarity of the structure in the CuI matrix (Figure 2c). Covalent P–P bonds are tilted such that a P_5 ring changes from a half-chair into an envelope conformation. In the CuI matrix, this part is fixed by Cu, that is, Cu determines the structure through the coordination to two P atoms. A rather helical arrangement is converted into a linear unit, which enables better packing and increased space filling.

The structural parameters of the three nanorod forms before and after the extraction are compared in Table 1. While the cell geometry changes when the matrices are removed, the translational periods of the polymers should remain virtually unchanged. They are in fact very well reproduced by the calculations (deviations about 1–2%). Owing to the good agreement with available experimental data, the calculated nanorod structures and the stability order of these and all other previously known crystalline P allotropes can be assumed to be valid.

Table 1: Lattice parameters of the crystal structures of the P nanorods with (experimental, $T = 298$ K) and without (calculated with GGA-D2, $T = 0$ K) CuI matrices. The symbols β and t correspond to the monoclinic angle and the translation period.

	$(CuI)_8P_{12}$	[P8]P4(4)[	$(CuI)_3P_{12}$	[P10]P2[	$(CuI)_2P_{14}$	[P12]P2[
SG (No.)	$P2_1/c$ (14)		$P2_1$ (4)		$P2_1/c$ (14)	
a [Å]	15.34	9.47	12.85	12.96	9.92	7.01
b [Å]	12.93	10.61	13.86	14.16	9.72	11.43
c [Å]	15.26	11.25	9.65	6.48	16.48	16.64
β [°]	116.4	99.7	109.4	105.1	105.7	114.4
V [Å^3]	2711.1	1114.2	1620.1	1034.3	1529.0	1214.2
t [Å]	16.13	15.87	13.86	14.16	16.48	16.64

The calculated structures of the isolated nanorods can be used to explain even the previously not understood experimental diffractograms of [P8]P4(4)[and [P10]P2[. They are plotted in Figure 3 along with the simulated diffraction patterns of the optimized crystal structures. Due to the conformity of the positions of the strongest reflections, the preservation of the tubular units and the occurrence of packings according to the simulations can be concluded. A significant agglomeration or polymerization to larger aggregates can be excluded as a result of the large peak broadening. The simulation of the diffraction patterns with strongly broadened reflections well reproduces the experiment.

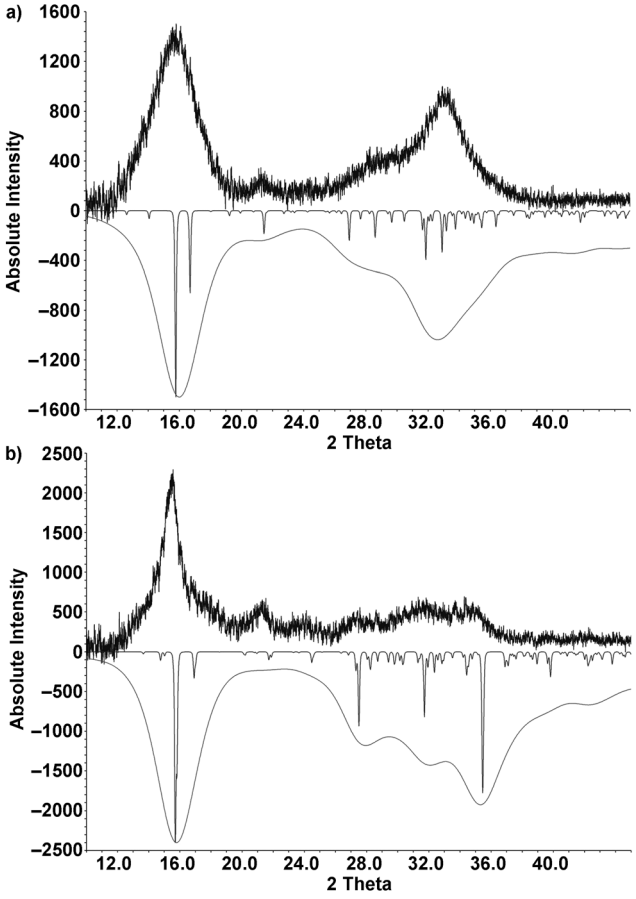

Figure 3. Powder diffraction patterns of isolated polymers of a) [P8]P4(4)[(extracted from $(CuI)_8P_{12}$) and b) [P10[P2 [(from $(CuI)_3P_{12}$). The diffractograms of the structures calculated with GGA-D2 ($T = 0$ K) are displayed below the abscissa and additionally widened for better comparability (the half-widths are increased from 0.1 to 3°).

The obtained results show that van der Waals forces are not only responsible for keeping together the molecular units in the allotropes of phosphorus but also for explaining the thermodynamic stability of black phosphorus. Experimental data were reproduced correctly when van der Waals interactions were taken into accounn with GGA-D2 in contrast to the result obtained with standard DFT methods, and a plausible stability sequence of all allotropes could be calculated.

Among the energetically closely located allotropes, black phosphorus is confirmed to be the thermodynamically stable form at 0 K. Models for the crystal structures of tubular P nanorods could be attained for the first time. They confirm that single P nanorods actually exist in Pfitzner's new allotropes, which are held together by strong van der Waals forces. The models also explain not-yet-understood structural features in $(CuI)_2P_{14}$. The successful description of the entire set of known P allotropes—with large structural and minimal energetic differences—emphasizes the importance of new developments for precise calculations such as the Grimme correction used here. These methods are being improved continuously (e.g. DFT-D3 for heavier elements),[19] can be combined with other functional approaches, and their scope extends to many other fields of chemistry, in which van der Waals interactions play an important role.[20,25]

Experimental Section

The syntheses of $(CuI)_8P_{12}$ and $(CuI)_3P_{12}$ as well as the isolation of the P nanorods and their characterization are described in Ref. [9,11,12].

X-ray powder patterns were obtained with a Huber G670 camera with Cu-Kα_1 radiation. Samples were attached to a Mylar foil with glue. Further details on the crystal structure investigations may be obtained from the Fachinformationszentrum Karlsruhe, 76344 Eggenstein-Leopoldshafen, Germany (fax: (+49) 7247-808-666; e-mail: crysdata@fiz-karlsruhe.de), on quoting the depository numbers CSD-203233 to -203242.

The quantum mechanical calculations were carried out within the framework of DFT with exchange-correlation functionals in the generalized gradient approximation (GGA) according to Perdew–Burke–Enzerhof (PBE)[21] and in the local density approximation (LDA) according to Perdew and Wang.[22] Crystal structures and energies were additionally calculated by means of the semiempirical long-range dispersion correction by Grimme (GGA-D2).[15] All calculations were executed with the Vienna Ab initio Simulation Package (VASP).[23] Atomic site parameters and cell constants were therefore allowed to fully relax within the conjugant gradient algorithm. The interactions between ions and electrons were described by the projector-augmented-wave method (PAW)[24] with a cutoff energy of 500 eV. A structure optimization was considered to be converged with a difference in total energy of less than 1×10^{-6} eV and a maximum Hellmann–Feynman force of 1×10^{-4} eV Å^{-1}. The final values of the total energies of the investigated systems were obtained with energy differences (between last and second to last step) of less than 1×10^{-3} eV per formula unit.

Received: April 9, 2014
Revised: June 6, 2014
Published online: September 5, 2014

Keywords: density functional calculations · phosphorus · structure elucidation · van der Waals interactions

[1] A. F. Holleman, E. Wiberg, N. Wiberg, *Lehrbuch der anorganischen Chemie*, de Gruyter, **1995**.

[2] a) C. Feldmann, *Angew. Chem.* **2013**, *125*, 7762; *Angew. Chem. Int. Ed.* **2013**, *52*, 7610; b) N. Pienack, W. Bensch, *Angew. Chem.* **2011**, *123*, 2062; *Angew. Chem. Int. Ed.* **2011**, *50*, 2014; c) M. Jansen, J. C. Schön, *Angew. Chem.* **2006**, *118*, 3484; *Angew. Chem. Int. Ed.* **2006**, *45*, 3406; d) M. Jansen, I. V. Pentin, J. C. Schön, *Angew. Chem.* **2012**, *124*, 136; *Angew. Chem. Int. Ed.* **2012**, *51*, 132.

[3] H. Okudera, R. E. Dinnebier, A. Simon, *Z. Kristallogr.* **2005**, *220*, 259.

[4] For reasons of simplicity, the known crystalline compounds are subsequently distinguished according to their crystal systems (o = orthorhombic black P, h = trigonal–rhombohedral high-pressure P, c = cubic high-pressure P, m = monoclinic violet P (Hittorf), t = triclinic fibrous P(Ruck)); the nanorods are described more accurately later in the text based on Baudler's notation.

[5] a) S. Lange, P. Schmidt, T. Nilges, *Inorg. Chem.* **2007**, *46*, 4028; b) T. Nilges, M. Kersting, T. Pfeifer, *J. Solid State Chem.* **2008**, *181*, 1707.

[6] R. Ahuja, *Phys. Status Solidi B* **2003**, *235*, 282.

[7] a) W. L. Roth, T. W. DeWitt, A. J. Smith, *J. Am. Chem. Soc.* **1947**, *69*, 2881; b) M. Rubenstein, F. M. Ryan, *J. Electrochem. Soc.* **1966**, *113*, 1063; c) V. V. Nechaeva, N. D. Talanov, A. I. Soklakov, *Zh. Neorg. Khim.* **1979**, *24*, 1979.

[8] H. Thurn, H. Krebs, *Acta Crystallogr. Sect. B* **1969**, *25*, 125.

[9] A. Pfitzner, M. F. Bräu, J. Zweck, G. Brunklaus, H. Eckert, *Angew. Chem.* **2004**, *116*, 4324; *Angew. Chem. Int. Ed.* **2004**, *43*, 4228.

[10] a) M. Ruck, D. Hoppe, B. Wahl, P. Simon, Y. Wang, G. Seifert, *Angew. Chem.* **2005**, *117*, 7788; *Angew. Chem. Int. Ed.* **2005**, *44*, 7616; b) A. Pfitzner, *Angew. Chem.* **2006**, *118*, 714; *Angew. Chem. Int. Ed.* **2006**, *45*, 699.

[11] M. H. Möller, W. Jeitschko, *J. Solid State Chem.* **1986**, *65*, 178.

[12] a) A. Pfitzner, E. Freudenthaler, *Angew. Chem.* **1995**, *107*, 1784; *Angew. Chem. Int. Ed. Engl.* **1995**, *34*, 1647; b) A. Pfitzner, E. Freudenthaler, *Z. Naturforsch. B* **1997**, *52*, 199.

[13] S. Böcker, M. Häser, *Z. Anorg. Allg. Chem.* **1995**, *621*, 258.

[14] a) M. Baudler, *Angew. Chem.* **1982**, *94*, 520; *Angew. Chem. Int. Ed. Engl.* **1982**, *21*, 492; b) M. Baudler, *Angew. Chem.* **1987**, *99*, 429; *Angew. Chem. Int. Ed. Engl.* **1987**, *26*, 419; c) M. Baudler, K. Glinka, *Chem. Rev.* **1993**, *93*, 1623; d) Simply put, repeating units of polymer structures are divided into polyhedral fragments and bridging links. Polyhedra are enclosed by square brackets in Baudler's notation.

[15] a) O. Osters, T. Nilges, F. Bachhuber, F. Pielnhofer, R. Weihrich, M. Schöneich, P. Schmidt, *Angew. Chem.* **2012**, *124*, 3049; *Angew. Chem. Int. Ed.* **2012**, *51*, 2994; b) N. Eckstein, A. Hohmann, R. Weihrich, T. Nilges, P. Schmidt, *Z. Anorg. Allg. Chem.* **2013**, *639*, 2741.

[16] S. Grimme, *J. Comput. Chem.* **2006**, *27*, 1787.

[17] M. E. Schlesinger, *Chem. Rev.* **2002**, *102*, 4267.

[18] P. A. G. O'Hare, B. M. Lewis, I. Shirotani, *Thermochim. Acta* **1988**, *129*, 57.

[19] S. Grimme, J. Antony, S. Ehrlich, H. Krieg, *J. Chem. Phys.* **2010**, *132*, 154104.

[20] a) A. J. Karttunen, T. F. Faessler, *Chem. Eur. J.* **2014**, *20*, 6693; b) S. Appalakondaiah, G. Vaitheeswaran, S. Lebègue, N. E. Christensen, A. Svane, *Phys. Rev. B* **2012**, *86*, 035105.

[21] a) J. P. Perdew, K. Burke, M. Ernzerhof, *Phys. Rev. Lett.* **1996**, *77*, 3865; b) J. P. Perdew, K. Burke, M. Ernzerhof, *Phys. Rev. Lett.* **1997**, *78*, 1396.

[22] a) J. P. Perdew, A. Zunger, *Phys. Rev. B* **1981**, *23*, 5048; b) J. P. Perdew, Y. Wang, *Phys. Rev. B* **1992**, *45*, 13244.

[23] a) G. Kresse, *J. Non-Cryst. Solids* **1995**, *193*, 222; b) G. Kresse, J. Hafner, *Phys. Rev. B* **1994**, *49*, 14251; c) G. Kresse, J. Furthmüller, *Comp. Mater. Sci.* **1996**, *6*, 15; d) G. Kresse, J. Furthmüller, *Phys. Rev. B* **1996**, *54*, 11169.

[24] a) P. E. Blöchl, *Phys. Rev. B* **1994**, *50*, 17953; b) G. Kresse, D. Joubert, *Phys. Rev. B* **1999**, *59*, 1758.

[25] After this manuscript had been submitted a number of papers appeared in which *o*-P is reported as single and multiple layers in "phosphorus": L. Li, Y. Yu, G. J. Ye, Q. Ge, X. Ou, H. Wu, D. Feng, X. H. Chen, Y. Zhang, *Nature Nanotechnol.* **2014**, *9*, 372; H. O. H. Churchill, P. Jarillo-Herrero, *Nature Nanotechnol.* **2014**, *9*, 330; H. Liu, A. T. Neal, Z. Zhu, Z. Luo, X. Xu, D. Tománek, P. D. Ye, *ACS Nano*, **2014**, *8*, 4033.

